# Ionophoric Activity of Pluronic Block Copolymers†

Oxana O. Krylova§ and Peter Pohl*,§,‡

*Forschungsinstitut für Molekulare Pharmakologie, Campus Berlin-Buch, Robert-Roessle Strasse 10, 13125 Berlin, Germany, and Lehrstuhl für Experimentelle Biophysik, Institut für Biologie, Humboldt-Universitaet, Invalidenstrasse 43, 10115 Berlin, Germany*

*Received October 1, 2003; Revised Manuscript Received January 6, 2004*

ABSTRACT: Pluronic block copolymers (triblock copolymers of poly(ethylene oxide) and poly(propylene oxide)) exhibit a chemosensitizing effect on multidrug resistant cell lines. Changes in membrane permeability are hypothesized to be responsible because inhibition of drug transport mediated by both the multidrug-resistance-associated protein and the P-glycoprotein drug efflux system has been observed. To test this hypothesis, we now have studied the ion conductivity mediated by Pluronic L61. Besides a detergent-like action, the copolymer was able to form regular channels and to exhibit carrier activity. Long living ion channels were formed by polymer oligomerization. Aggregate equilibrium was shifted toward L61 monomers and dimers, which operated as mobile carriers. Copolymer-induced membrane permeability for potassium ions (1 M KCl) was less than $10^{-8}$ cm $s^{-1}$, whereas the permeability for uncharged doxorubicin molecules (1 mM) was equal to $5 \times 10^{-4}$ cm $s^{-1}$. The results are consistent with reports about an increased doxorubicin accumulation in cells (Venne, Li, S., Mandeville, R., Kabanov, A., and Alakhov, V. Y. (1996) *Cancer Res. 56*, 3626−3629). However, the increased permeability contrasts with the polymer-mediated decrease of drug efflux from cells. Preferential polymer binding to membrane proteins may mask the unspecific effect of L61 observed on lipid bilayers.

Multidrug resistance (MDR)[1] is often associated with overexpression of both multidrug-resistance-associated protein (MRP) and P-glycoprotein drug efflux system (P-gp). These proteins are assumed to be responsible for the lack of drug accumulation and retention in tumor cells (*1*−*4*).

In the presence of Pluronics, the cytotoxic activity of chemotherapeutic agents against drug resistant cells increases up to 1000 times, whereas only marginal changes in their activity are observed in the case of sensitive cells (*5*−*7*). Similarities in the effects of copolymers on MRP and P-gp drug efflux systems led to the suggestion that a single unifying mechanism may explain the inhibition (*8*). Contrasting reports about specific polymer interactions with MRP and P-gp (*9*, *10*) have questioned this hypothesis. Nevertheless, unspecific effects of block copolymers exist, and without knowledge of the underlying mechanism it is impossible to conclude whether they contribute to the reversal of drug resistance. Pluronics, for example, promote drug penetration across membrane barriers (*11*−*13*), cause water-soluble dyes to leak from liposomes (*14*), and facilitate transmembrane fatty acid transport (*13*). Structurally related octablock copolymers of poly(ethylene oxide) and poly(propylene oxide) increase the influx of $Na^+$ and the efflux of $K^+$ from human erythrocytes (*15*).

The molecular mechanism by which Pluronics increase membrane permeability is still unknown. Disturbance of membrane structure and integrity is likely because the hydrophobic (central) part of some Pluronics is long enough to span the bilayer. In the current study, Pluronic L61 (kindly provided by BASF) has been used. We have found that L61 (Figure 1) is able to act as a mobile carrier and as an ion channel as well. Its mode of action depends on the level of aggregation. Whereas the carrier is formed by the L61 monomers or dimers, channels are likely to be formed by oligomers.

## MATERIALS AND METHODS

*Chemicals.* Diphytanoylphosphatidylcholine (DPhPC) was obtained from Avanti Polar Lipids (Alabaster, AL) and used without further treatment. The components of buffer solutions, HEPES, MES, Tris, choline chloride, and KCl, the anticancer drug doxorubicin, and all organic solvents were from Fluka. The copolymer L61 was a gift from BASF. Polymer polydispersity was smaller than 1.1.

*Membrane Binding of Doxorubicin.* Upon binding to large unilamellar vesicles (LUVs), doxorubicin (Figure 1) introduces a surface charge to the initially uncharged DPhPC bilayer. In turn, the surface charge increases the electrophoretic mobility of LUVs. The velocity, $v$, of vesicle movement in an electrical field was measured by a $\zeta$-sizer (model DELSA 440 SX, Coulter Electronics, Inc., Hialeah,

† Work was supported by the Volkswagenstiftung (Grant I/77743) and the Deutsche Forschungsgemeinschaft (Grant Po 533/7-1).

* To whom correspondence should be addressed: e-mail pohl@fmp-berlin.de; fax +49 30 94793 291; tel +49 30 94793 283.

‡ Humboldt-Universitaet.

§ Forschungsinstitut für Molekulare Pharmakologie.

[1] Abbrevations: MDR, multidrug resistance; MRP, multidrug-resistance-associated protein; P-gp, P-glycoprotein; DPhPC, diphytanoylphosphatidylcholine; LUVs, large unilamellar vesicles; $\delta$, thickness of the near-membrane unstirred layer; $P_{UL}$, unstirred layer permeability; $P_M$, membrane permeability; $\psi_s$, membrane surface potential; $\psi_b$, membrane boundary potential; $\Delta\psi_s$, interleaflet difference of membrane surface potential; $\Delta\psi_b$, interleaflet difference of membrane boundary potential.

10.1021/bi035768l CCC: $27.50 
Published on Web 03/03/2004

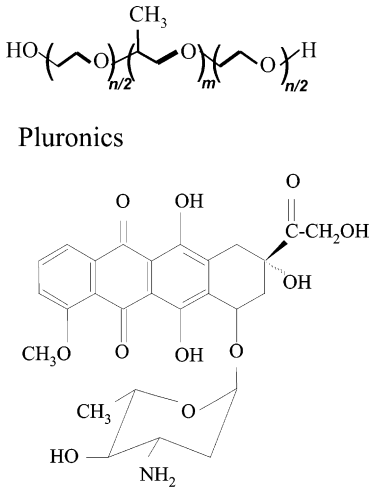


FIGURE 1: Structure of Pluronics and doxorubicin. Pluronic L61 consists of a large hydrophobic block ($m = 30$) enclosed between two small hydrophilic blocks ($n = 4$). Doxorubicin is a weak base that at physiological pH values is positively charged. The drug is able to translocate through membranes in its uncharged form.

FL) with a four-beam electrophoretic laser scattering analyzer and used to calculate the electrical potential, $\zeta$, at the shear plane. This plane defining what migrates in the electric field is about 0.2−0.4 nm beyond the charged vesicle surface (*16*). The magnitude of the $\zeta$-potential is, thus, less than the surface potential of the outer membrane leaflet, $\psi_{s,cis}$, and it is related to $\psi_{s,cis}$ by the Gouy−Chapman theory (*17*−*19*).

LUVs were prepared from a thin DPhPC film made by solvent evaporation from a lipid−chloroform solution. Buffer addition led to the formation of multilamellar vesicles. Subsequent extrusion (*20*) by the small-volume apparatus LiposoFast (Avestin Inc., Ottawa, Canada) equipped with filters of 100 nm pore diameter resulted in unilamellar vesicles. The final lipid concentration was 1 mg/mL.

*Formation of Planar Membranes.* Two different methods were used to form planar lipid bilayers: (i) Planar black lipid membranes were formed from a 20 mg/mL solution of DPhPC in *n*-decane (*21*). They were spread across a circular aperture (0.7 mm in diameter) in a diaphragm separating two aqueous phases of a Teflon chamber. (ii) The monolayer apposition technique (*22*, *23*) was used to form solvent-free membranes across an aperture (130−180 $\mu$m in diameter) in a Teflon septum (thickness 25 $\mu$m) separating two aqueous compartments. The septum was pretreated with a 2% solution of hexadecane in hexane. On top of the two aqueous phases, a 20 mg/mL solution of lipid in hexane was spread to form lipid monolayers. After solvent evaporation, the buffer solution levels in both compartments were raised above the aperture by syringes. Within the aperture, the two monolayers combined spontaneously to a bilayer.

In both cases, the buffer solution was agitated by magnetic bars. The experiments were carried out at room temperature (21−23 °C).

*Measurements of Transmembrane Current and Single-Channel Activity.* The current was monitored under voltage clamp conditions. Therefore Ag/AgCl reference electrodes were immersed into the bathing buffer solutions at both sides of the membrane. The recording filter of the current amplifier (model VA-10, NPI Electronic, Tamm, Germany) was a three-pole Bessel low-pass filter with a corner frequency of 100 Hz. The amplified signal was digitalized by a PCI 6025E computer board (National Instruments, Muenchen, Germany) and analyzed by the WINEDR software package (Strathclyde Electrophysiology Software, Strathclyde, U.K.). Gaussian filters between 1 and 7 Hz were applied to reduce noise.

*Monitoring Doxorubicin Transport by Measurements of the Interleaflet Boundary Potential Difference, $\Delta\psi_b$.* The $\Delta\psi_b$ of the membrane originates from the interfacial differences in surface, $\Delta\psi_s$, and dipole, $\Delta\psi_d$, potentials. Surface potential and, thus, the boundary potential of the outer leaflet, $\psi_{s,cis}$ and $\psi_{b,cis}$, respectively, increase upon adsorption of the positively charged doxorubicin. Transmembrane permeation of doxorubicin and its subsequent adsorption to the inner monolayer tend to increase also the respective potentials $\psi_{s,trans}$ and $\psi_{b,trans}$ of the inner monolayer. Thus, $\Delta\psi_b = \psi_{b,cis} - \psi_{b,trans}$ is a measure of the transmembrane concentration difference (*24*) and can be used to monitor doxorubicin transport. We have measured $\Delta\psi_b$ by capacitance minimization (*25*). At its minimum, the capacitive current does not contain a signal harmonic to the fundamental frequency (*26*). In our setup (*19*, *24*), the second harmonics of the amplified current is detected by a lock-in amplifier (model 7265, Perkin Elmer, Shelton, CT). The dc offset required to minimize the amplitude of the overtone is adjusted every second and applied along with the sine voltage to the membrane (source, model 33120A, Hewlett-Packard, Loveland, CO). It is equal in magnitude to $\Delta\psi_b$ but opposite in sign.

## RESULTS

*Pluronic L61 Does Not Alter Doxorubicin Adsorption to the Lipid Bilayer.* Adsorption of the positively charged cytotoxic drug doxorubicin to the outer (cis) leaflet of LUVs resulted in a change of membrane surface potential, $\Delta\psi_{s,cis}$ (Figure 2A,B). Particle electrophoresis revealed a saturation of binding places at high doxorubicin concentrations. Both in the presence and in the absence of the copolymer, the same $\Delta\psi_{s,cis}$ was measured at any particular doxorubicin concentration. Even at very high concentrations, the polymer did not affect $\Delta\psi_{s,cis}$ (Figure 2A,B).

At corresponding doxorubicin concentrations, $\Delta\psi_b$ and $\Delta\psi_{s,cis}$ obtained on planar bilayers and LUVs, respectively, were identical. Since $\Delta\psi_b$ represents the sum of $\Delta\psi_s$ and $\Delta\psi_d$, it is concluded that doxorubicin does not change membrane dipole potential. The result indicates that, most probably, doxorubicin adsorbs only to the outer plane of the bilayer. Alternatively, a binding site closer to the membrane center may be compatible with the results, provided the doxorubicin dipole moment adopts an orientation parallel to the plane of the membrane.

*Effect of Pluronic L61 on the Transmembrane Movement of Doxorubicin.* In the presence of a pH gradient, the uncharged form of doxorubicin permeates the membrane (*27*); that is, it deprotonates at the first interface, diffuses through the membrane, and picks up another proton at the second leaflet. Commonly, the permeability of planar bilayers for weak acids and bases requires the diffusion through near-membrane stagnant water layers to be taken into account (*28*). Representing additional transport barriers, the cis and trans unstirred layers (UL) have the same thickness, $\delta$, and

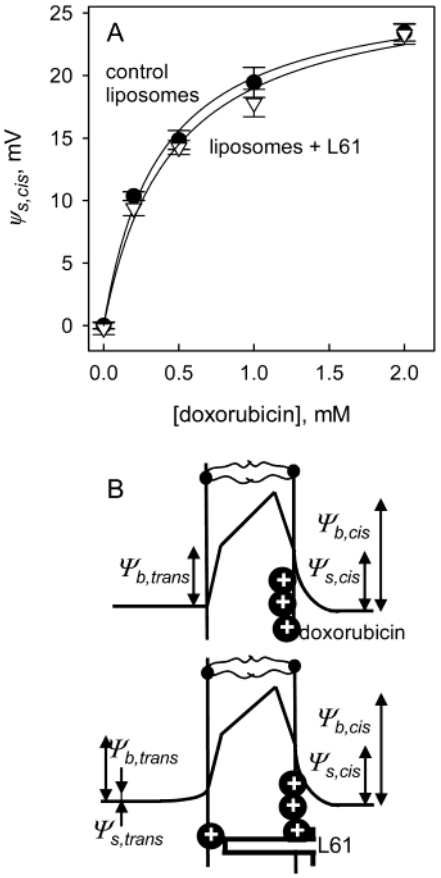


FIGURE 2: Changes of surface potential, $\psi_{s,cis}$, caused by doxorubicin adsorption to the surface of large unilamellar lipid vesicles. Panel A shows representative experimental records. Both in the absence (●) and in the presence of 50 $\mu$M L61 (▽), doxorubicin gave rise to the same surface potential of the outer membrane leaflet, $\psi_{s,cis}$. The final lipid concentration was 0.5 mg/mL. The buffer contained 10 mM HEPES, 10 mM Tris, and 20 mM choline chloride, pH 7.5. Panel B shows a scheme of membrane surface and boundary potentials. Adsorption of doxorubicin to the outer leaflet determines $\psi_{s,cis}$. Eventual doxorubicin translocation mediated by the polymer L61 does not alter $\psi_{s,cis}$ because the $\zeta$-potential measurements are made after the system has been allowed to equilibrate and because the internal volume of the vesicles is small compared to the total volume of the suspension.

thus, the same permeability, $P_{UL}$:

$$P_{UL,cis} = P_{UL,trans} = P_{UL} = D/\delta = 2 \times 10^{-6}\,cm^2\,s^{-1}/0.02\,cm = 10^{-4}\,cm\,s^{-1} \quad (1)$$

The conservation of mass requires the doxorubicin flux through the membrane to be equal to its flux through the unstirred layers in the immediate membrane vicinity:

$$J = P_{UL}(c_{cis} - c_{cis,m}) = P_M\frac{K_D}{[H^+]}(c_{cis,m} - c_{trans,m}) = P_{UL}(c_{trans,m} - c_{trans}) \quad (2)$$

where $c_{cis}$, $c_{trans}$, $c_{cis,m}$, and $c_{trans,m}$ are the bulk and near-membrane concentrations of the doxorubicin cation in the cis and trans compartments, respectively (Figure 3C). The index cis denotes the compartment containing doxorubicin. Since the dissociation constant ($K_D = 10^{-8.6}$ M) is much smaller than the proton concentration ([H$^+$] = $10^{-7.5}$ M), the diffusion of neutral doxorubicin molecules through the

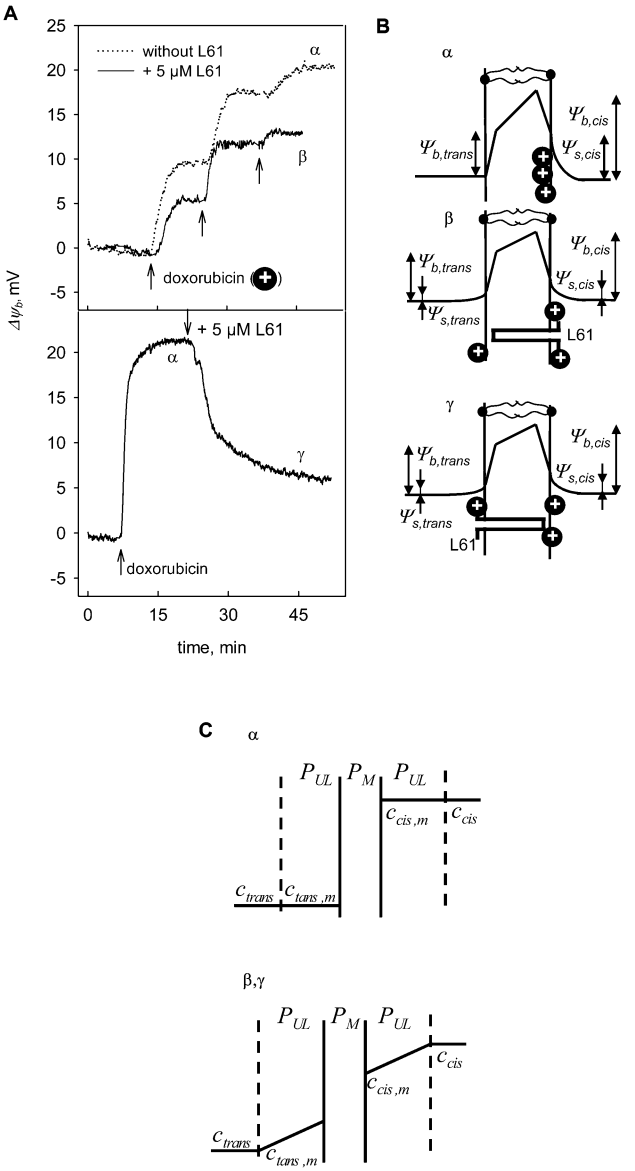


FIGURE 3: Interleafleat boundary potential difference, $\Delta\psi_b$, induced by unilateral addition of doxorubicin to a planar bilayer lipid membrane. The bilayer was formed from a DPhPC solution in *n*-decane (*21*). In part A, upper panel, upward arrows indicate the addition of doxorubicin in final aqueous cis concentrations of 0.1, 0.5, and 1 mM (dotted line). The experiment was repeated in the presence of 5 $\mu$M L61 (solid line) in the cis compartment. In part A, lower panel, 1 mM doxorubicin was added to the cis compartment (upward arrow). After $\Delta\psi_b$ has reached a stationary value, 5 $\mu$M L61 was added to the trans compartment. For buffer composition, see Figure 2. Labels α, $\beta$, and $\gamma$ indicate three different steady-state conditions. Part B shows a scheme of membrane surface and boundary potentials. In the upper panel, there is no difference in doxorubicin adsorption to planar bilayers and vesicles (compare Figure 2). In the middle panel, the polymer L61 added to the cis compartment facilitates doxorubicin translocation trough the membrane. The interleaflet boundary and surface potential differences, $\Delta\psi_b = \psi_{b,cis} - \psi_{b,trans} = \Delta\psi_s = \psi_{s,cis} - \psi_{s,trans}$, decrease due to the adsorption of doxorubicin to the trans leaflet. In the lower panel, when located in the trans compartment, L61 mediates doxorubicin permeation as effectively as it does in the cis compartment. Part C shows the steady-state doxorubicin concentration profiles in the unstirred layers adjacent to the planar bilayer. In the upper panel, in the absence of L61 the membrane permeability $P_M$ is much smaller than the permeability $P_{UL}$ of the near-membrane unstirred layers. In the lower panel, L61 augments $P_M$ so that $P_M$ and $P_{UL}$ are of the same order of magnitude.

unstirred layer has been neglected. Calculation of the transmembrane flux is based on the assumption that doxorubicin permeates the membrane in its uncharged form (*27*) and that the deprotonation reaction is much faster than the translocation through the membrane. Because of the bulkiness of the compartments, $c_{trans}$ is assumed to be zero during all experiments. From eq 2 follows that

$$c_{cis} - c_{cis,m} = c_{trans,m} = \Delta c_{UL} \quad (3)$$

and that

$$\frac{P_{UL}}{0.1P_M} = \frac{\Delta c_M}{\Delta c_{UL}} \quad (4)$$

where $\Delta c_M$ is the transmembrane doxorubicin concentration difference. Since changes of $\Delta c_M$ are indicated by alterations of $\Delta\psi_s$ (Figure 2A, B), boundary potential measurements can be used to assess $P_M$ (*19*, *24*).

In the absence of L61, the interfacial doxorubicin concentrations on both sides of the membrane are very close to the respective bulk concentrations (Figure 3C). This result is derived from the observation that $\Delta\psi_b$ (Figure 3A, upper panel) accurately matched the change $\Delta\psi_{s,cis}$ induced by doxorubicin adsorption (compare Figure 2A). From $\Delta c_{UL} \ll \Delta c_M$ follows according to eq 4 that $P_M \ll P_{UL}$. This result agrees well with a $P_M$ of $2 \times 10^{-6}$ cm s$^{-1}$ measured on red blood cells (*29*).

In the presence of L61, we observed $\Delta\psi_b < \Delta\psi_{s,cis}$ (Figure 3A,B). The induced drop of $\Delta\psi_b$ from 20 to 5.6 mV (Figure 3A, lower panel) indicated that $\psi_{cis}$ decreased from 20 to 17.8 mV and $\psi_{trans}$ increased from 0 to 12.2 mV (Figure 3B). This was the only combination of the two surface potentials matching the measured $\Delta\psi_b$ and satisfying eq 3. The corresponding values for $c_{cis,m}$ and $c_{trans,m}$ were 0.7 and 0.3 mM, respectively (compare Figure 2A). According to eq 4, $P_M = (0.3/0.4) \times 10^{-3}$ cm s$^{-1}$ $= 7.5 \times 10^{-4}$ cm s$^{-1}$. Thus, L61 facilitated doxorubicin transport when it was separated from doxorubicin by the membrane. The same result was obtained for the situation where doxorubicin and L61 were given to the cis compartment. At the final doxorubicin concentration in Figure 3A (upper panel), $\psi_{cis}$ and $\psi_{trans}$ were 18.7 and 7.1 mV, respectively, and the corresponding $c_{cis,m}$ and $c_{trans,m}$ amounted to 0.14 and 0.86 mM, respectively. Thus, $P_M$ was equal to $2 \times 10^{-4}$ cm s$^{-1}$. Seven more runs of the experiments in cis and trans configurations resulted in a $P_M$ of $(5 \pm 2) \times 10^{-4}$ cm s$^{-1}$.

Obviously, the polymer is able to cross the membrane and to form a complex with doxorubicin facilitating thereby doxorubicin diffusion. Alternatively, membrane-spanning segments of several polymer molecules may form a transmembrane pore that enables doxorubicin to cross the membrane. To establish the mechanism by which L61 facilitates membrane transport, we have carried out experiments in a voltage clamp configuration.

*Changes of Bilayer Conductivity Mediated by Pluronic L61.* Insertion of L61 into the planar bilayer was accompanied by a conductivity increase that consisted of segments with continuous growth and of segments with stepwise discrete jumps to higher conductance levels. Whereas the latter clearly demonstrated the formation of some transient pores, the former suggested ion transport according to the mechanism of mobile carriers (Figure 4). Commonly, a steady-state current was achieved within several minutes after polymer addition, and the membranes retained their stability within hours.

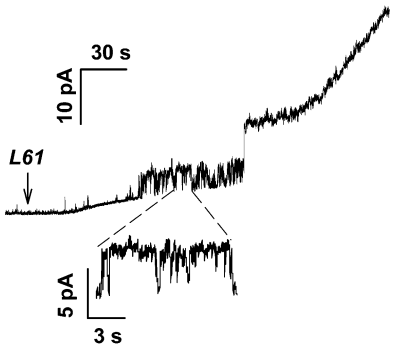


FIGURE 4: Time drive of membrane permeability increase induced by Pluronic L61. After the addition of 30 $\mu$M L61 (upward arrow) to the bathing buffer solutions on both sides of a solvent-free membrane, smooth rises in conductance and channel gatings were observed. The buffer contained 10 mM HEPES, 10 mM Tris, and 1 M KCl, pH 7.5. To reduce noise, a Gaussian filter of 7 Hz was applied.

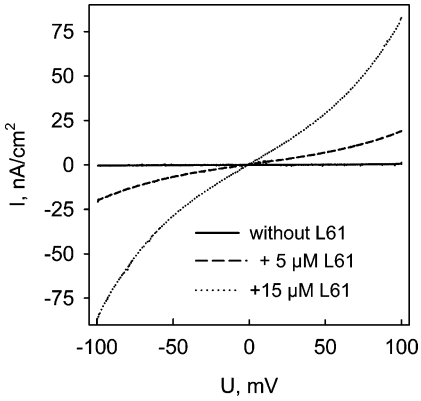


FIGURE 5: Current−voltage curves of the steady-state transmembrane current through a planar lipid bilayer in the absence L61 (solid line) and in its presence (dashed and dotted lines). The experimental conditions were similar to those in Figure 4. To reduce noise, a Gaussian filter of 1 Hz was applied.

Voltage−current dependencies of the steady-state current in Pluronic-containing media were nonlinear (Figure 5). The additional conductivity observed at higher voltages (>50 mV) was consistent with the view that the partition of the charged conducting polymer ion complex was facilitated by the electric field. Aqueous copolymer concentrations of 5 and 30 $\mu$M increased membrane conductivity (calculated for zero voltage) 40- and 700-fold, respectively.

Substitution of $K^+$ for $Ca^{2+}$ or for *N*-methyl-D-glucamine revealed that the substrate specificity of L61 is rather low. With a slightly diminished efficiency, L61 transports divalent cations and organic cations as well (Figure 6).

At lower salt concentration (300 mM), the Pluronic-induced membrane permeability was proportional to the copolymer concentration (Figure 7A, top) suggesting a polymer−ion ratio in the complex of 1:1. At high salt concentration (1 M), the stoichiometry is shifted toward a lower occupancy mode (Figure 7A, bottom). In addition to the complex of one L61 molecule and one ion, a conducting complex of two L61 molecules and one ion may be formed. This conclusion is based on the observation that membrane

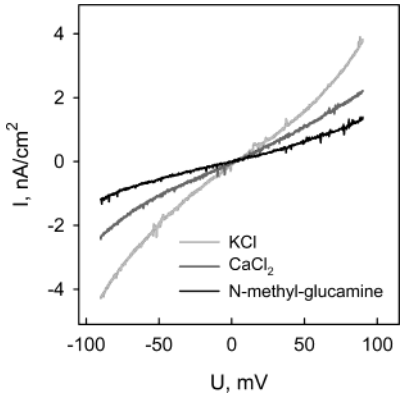


FIGURE 6: Low specificity of substrate binding by L61. In a concentration of 50 $\mu$M, the block copolymer carries KCl (light grey), $CaCl_2$ (grey), and *N*-methyl-D-glucamine (black). Dry DPhPC membranes (*22*, *23*) were surrounded by a buffer (pH 7.5) containing 10 mM HEPES, 10 mM Tris, and 300 mM of the corresponding salt. Their conductivities were, respectively, 2.3 and 35 nS/cm$^2$ (KCl), 2.5 and 19 nS/cm$^2$ ($CaCl_2$), and 1.2 and 14 nS/cm$^2$ (*N*-methyl-D-glucamine) in the absence and presence of L61. To reduce noise, a Gaussian filter of 1 Hz was applied.

conductivity can be fitted by an equation of the type $I = I_0 + ac + bc^2$, where $c$ is the polymer concentration, $I_0$ is the current in the absence of polymers, and $a$ and $b$ are constants. In the experiment shown in Figure 7A, bottom, $I$ was proportional to $c^{1.5}$. Multiple occupancy of the polymer carrier is also possible as suggested by the nonlinear dependence of membrane conductivity on KCl concentration (Figure 7B). The dilution potential measured via agar bridges indicates ideal cation selectivity of L61. The reversal potential of −17 mV was determined in a 2-fold KCl gradient (Figure 8).

Demonstration of gating is usually regarded as proof for an ion channel mechanism. In rare cases (about 10% of all records), reproducible time-dependent activation and deactivation of Pluronic-induced ion currents have been observed (Figure 9). Along with transitions between discrete conductivity levels, fast flickering spikes and irregular current fluctuations were detected (Figure 9). Whereas the latter indicates a detergent-like mode of action, "normal" channels are characterized by open times from several seconds up to 2−3 min and by a broad spectrum of amplitudes that in 1 M KCl ranged from 20 pS to 1 nS. If present at all, the detergent-like activity was observed at the beginning of the experiments (Figure 9, top traces). Sometimes only the carrier mode (Figure 5) or a combination of carrier and channel modes of action (Figures 4 and 8) were observed. Based on Ohm's law and assuming that the channel is a cylindrical pore, estimated pore diameters varied between 2 and 9 Å (for pore length of 50 Å and a conductivity of 110 mS/cm).

## DISCUSSION

Interacting with bilayer lipid membranes, Pluronics exhibit ionophoric activity and are able to facilitate transmembrane movement of a neutral drug. In part, this activity may contribute to the reversal of multidrug resistance that so far was attributed to its inhibitory action on both P-gp (*30*, *31*) and MRP (*8*, *12*). The nonspecific mode of action on the lipid matrix is consistent with the fact that different proteins are involved (*8*). Moreover, the results on lipid bilayers agree well with the observation that Pluronics decrease transepithelial electrical resistance to about 80% of initial values (*32*). Using a simple model system, we were now able to show that the conductivity increase is due to direct interactions of the polymer with the membrane. It occurs in three different modes (Figure 9). (1) Detergent mode: Insertion of the hydrophobic (central) block into the membrane is accompanied by defect formation; that is, the integrity of the membrane barrier is disturbed. Differences in the amplitude of current flickers are due to differences in the number of polymer molecules that insert at once. Corresponding irregular fluctuations of the transmembrane current are demonstrated in Figure 9. Numerous detergents, such as sodium dodecylsulfate, dodecyltriphenylphosphonium bromide, and dodecyltrimethylammonium bromide, disturb the lipid matrix in a similar way (*33*, *34*). (2) Carrier mode: Different from a detergent-like mode of action is the conductivity increase that occurs in the absence of current fluctuation and in the absence of any additional noise. The dependence of the current on polymer and ion concentrations indicates that both polymer monomers and dimers are involved. They form complexes with cations, thereby facilitating their movement

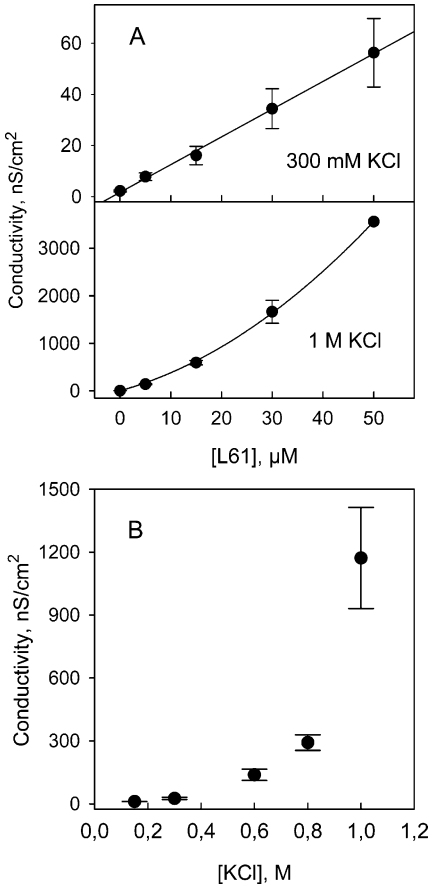


FIGURE 7: Stoichiometry of polymer cation complexes. Part A shows the dependence of membrane conductivity, $G$, on L61 concentration. The linear dependence of $G$ on L61 concentration suggested a 1:1 complex at low ionic strength (top). At higher salt concentrations (1 M KCl), complexes of different stoichiometry were formed as indicated by the observation that $G$ was proportional to $[L61]^{1.5}$ (bottom). Part B shows the nonlinear dependence of $G$ on the aqueous KCl concentration suggesting that multiple occupancy of a polymer carrier is also possible. The membrane conductivity values were calculated from voltage−current curves measured in the presence of 30 $\mu$M L61 added to both sides of the membrane. All other experimental conditions were similar to those in Figure 4.

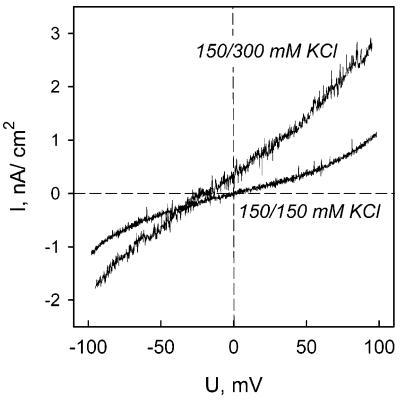


FIGURE 8: Cation selectivity of L61. The current−voltage curves were measured at an aqueous concentration of 50 $\mu$M L61. The transmembrane KCl concentration gradient of 150/300 mM yielded a reversal potential of −17 mV indicating ideal cation selectivity. Potentials were given with respect to the hyperosmotic solution; the hypoosmotic compartment was kept electrically at ground. To reduce noise, a Gaussian filter of 1 Hz was applied.

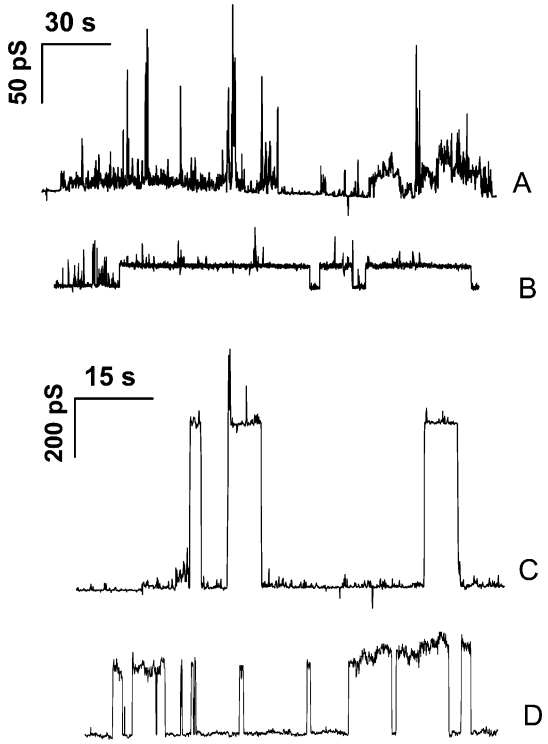


FIGURE 9: Representative recordings of L61 channel activity in 1 M KCl. Both irregular current fluctuations and regular ion channels of various sizes have been observed. Corresponding copolymer concentrations and applied voltages were (A) 15 $\mu$M and +60 mV, (B) 15 $\mu$M and −90 mV, (C) 15 $\mu$M and +50 mV, and (D) 3.5 $\mu$M and +50 mV. To reduce noise, a Gaussian filter of 7 Hz was applied.

through the membrane. (3) Channel mode: There is no sharp border to the detergent-like mode of action. The term channel mode is introduced to underline that regular openings and closings at distinct conductance levels occur, a feature that is not common for most detergents and carriers. Transmembrane channels are formed by larger polymer aggregates. Their size is determined by the number of Pluronics (and lipid molecules) involved. In most experiments, channel contribution to the total membrane conductance was rather low. Rare openings indicate that aggregate equilibrium is shifted toward polymer monomers and dimers (carrier mode).

Table 1

| | $P_M$ (cm s$^{-1}$) in the absence of L61 | $P_M$ (cm s$^{-1}$) in the presence of L61 | |
|---|---|---|---|
| | | carrier mode | channel mode |
| doxorubicin (1 mM) | $2 \times 10^{-6}$ [a] | $5 \times 10^{-4}$ | |
| KCl (1 M) | $8 \times 10^{-13}$ | $1.6 \times 10^{-10}$ | $9 \times 10^{-9}$ |

[a] Taken from ref *29*.

The size of the channels is sufficient to conduct small cations, but it is too small to provide a pathway for the larger doxorubicin molecules as well. Total L61-mediated ion conductivity $G = 600$ nS cm$^{-2}$ measured at a KCl concentration $c = 1$ M (Figure 7A) corresponds to a $P_M$

$$P_M = \frac{RT}{cz^2F^2}G$$

of $1.6 \times 10^{-10}$ cm s$^{-1}$, where $R$, $T$, $z$, and $F$ have their usual meanings. This value is several orders of magnitude smaller than the $P_M$ estimated for doxorubicin (Table 1). The difference in cation and doxorubicin transport efficiencies is easily explained by the fact that doxorubicin is transported in its neutral form (*13*). The modest increase in ion conductivity agrees well with the observation that ethylene oxide/propylene oxide copolymers display a very low cytotoxicity (*32*, *35*, *36*). Also the observed channel activity is too rare to enhance the cytotoxicity significantly (Table 1). The opening of just one channel (single channel conductance of 500 pS in 1 M KCl) augmented $P_M$ to $9 \times 10^{-9}$ cm s$^{-1}$ (Figure 9).

The increase of drug permeability mediated by Pluronic L61 in our model system is in line with its effect on drug translocation from apical to basolateral in porcine kidney cells stably expressing P-gp (*9*). However, in the reverse direction (i.e., from basolateral to apical), the opposite effect was found (*9*). It cannot be explained with the effect Pluronic exerts on lipid bilayer permeability. The same holds for the Pluronic-mediated inhibition of drug efflux from Chinese hamster ovary cells (*6*). The ability of L61 to alter the activity of membrane proteins seems to mask its effect on the lipid matrix of the membrane. Preferential binding to MRP and P-gp would provide an explanation. So far no clear picture has emerged from literature data. Reports about specific protein binding (*9*, *10*) contrast with observations that the effect of Pluronics on MRP and P-gp is unspecific (*8*).

The interaction of L61 with the lipid matrix should result in an increased proton permeability that, in turn, should partially uncouple mitochondrial phosphorylation. Representing a possible reason for chemosensitization of MDR cells by Pluronic block copolymers (*36*, *37*), ATP depletion should be, in part, due to the ionophoric activity of L61.

Besides its importance for MDR, the ionophoric activity of Pluronics may hamper fluorescence measurements of intracellular ion concentrations in which the polymers are used to prevent the fluorescent dye from forming aggregates in aqueous media. For example, in the case of $Ca^{2+}$ measurements with fura-2, the use of Pluronics is recommended because micelles may impede the passage of the hydrophilic probe across cell membranes (*38*).

In summary, the present study shows that Pluronic L61 facilitates not only (neutral) drug transport but also ion

movement across bilayer lipid membranes. Although much smaller than doxorubicin permeability, induced ion permeability may contribute to MDR reversal by Pluronics, for example, by contributing to ATP depletion. Besides unspecific effects on the lipid matrix, specific interactions of the polymer with membrane proteins have to be taken into account to explain the hypersensitization of MDR cells by L61. Experimental modeling of these phenomena will be undertaken with bilayers containing reconstituted P-gp or MRP.

## ACKNOWLEDGMENT

We thank Dr. N. S. Melik-Nubarov for fruitful discussions.

## REFERENCES

1. Ambudkar, S. V., Dey, S., Hrycyna, C. A., Ramachandra, M., Pastan, I., and Gottesman, M. M. (1999) Biochemical, cellular, and pharmacological aspects of the multidrug transporter, *Annu. Rev. Pharmacol. Toxicol. 39*, 361−398.
2. Hipfner, D. R., Deeley, R. G., and Cole, S. P. (1999) Structural, mechanistic and clinical aspects of MRP1, *Biochim. Biophys. Acta 1461*, 359−376.
3. Borst, P., Evers, R., Kool, M., and Wijnholds, J. (2000) A family of drug transporters: The multidrug resistance- associated proteins, *J. Natl. Cancer Inst. 92*, 1295−1302.
4. Wijnholds, J. (2002) Drug resistance caused by multidrug resistance-associated proteins, *Novartis Found. Symp. 243*, 69−79.
5. Alakhov, V. Y., Moskaleva, E. Y., Batrakova, E. V., and Kabanov, A. V. (1996) Hypersensitization of multidrug resistant human ovarian carcinoma cells by pluronic P85 block copolymer, *Bioconjugate Chem. 7*, 209−216.
6. Venne, A., Li, S., Mandeville, R., Kabanov, A., and Alakhov, V. Y. (1996) Hypersensitizing effect of pluronic L61 on cytotoxic activity, transport, and subcellular distribution of doxorubicin in multiple drug-resistant cells, *Cancer Res. 56*, 3626−3629.
7. Munshi, N., Rapoport, N., and Pitt, W. G. (1997) Ultrasonic activated drug delivery from pluronic P-105 micelles, *Cancer Lett. 118*, 13−19.
8. Miller, D. W., Batrakova, E. V., and Kabanov, A. V. (1999) Inhibition of multidrug resistance-associated protein (MRP) functional activity with pluronic block copolymers, *Pharm. Res. 16*, 396−401.
9. Evers, R., Kool, M., Smith, A. J., van Deemter, L., de Haas, M., and Borst, P. (2000) Inhibitory effect of the reversal agents V-104, GF120918 and pluronic L61 on MDR1 Pgp-, MRP1- and MRP2-mediated transport, *Br. J. Cancer 83*, 366−374.
10. Bogman, K., Erne-Brand, F., Alsenz, J., and Drewe, J. (2003) The role of surfactants in the reversal of active transport mediated by multidrug resistance proteins, *J. Pharm. Sci. 92*, 1250−1261.
11. Kabanov, A. V., Chekhonin, V. P., Alakhov, V. Y., Batrakova, E. V., Lebedev, A. S., Melik-Nubarov, N. S., Arzhakov, S. A., Levashov, A. V., Morozov, G. V., and Severin, E. S. (1989) The neuroleptic activity of haloperidol increases after its solubilization in surfactant micelles. Micelles as microcontainers for drug targeting, *FEBS Lett. 258*, 343−345.
12. Batrakova, E. V., Li, S., Miller, D. W., and Kabanov, A. V. (1999) Pluronic P85 increases permeability of a broad spectrum of drugs in polarized BBMEC and Caco-2 cell monolayers, *Pharm. Res. 16*, 1366−1372.
13. Erukova, V. Y., Krylova, O. O., Antonenko, Y. N., and Melik-Nubarov, N. S. (2000) Effect of ethylene oxide and propylene oxide block copolymers on the permeability of bilayer lipid membranes to small solutes including doxorubicin, *Biochim. Biophys. Acta 1468*, 73−86.
14. Jamshaid, M., Farr, S. J., Kearney, P., and Kellaway, I. W. (1988) Poloxamer Sorption on Liposomes − Comparison with Polystyrene Latex and Influence on Solute Efflux, *Int. J. Pharm. 48*, 125−131.
15. Atkinson, T. P., Bullock, J. O., Smith, T. F., Mullins, R. E., and Hunter, R. L. (1988) Ion transport mediated by copolymers composed of polyoxyethylene and polyoxypropylene, *Am. J. Physiol. 254*, C20−C26.
16. Carnie, S., and McLaughlin, S. (1983) Large divalent cations and electrostatic potentials adjacent to membranes. A theoretical calculation, *Biophys. J. 44*, 325−332.
17. Volkov, A. G., Deamer, D. W., Tanelian, D. L., and Markin, V. S. (1996) Electrical double layers at the oil/water interface, *Prog. Surf. Sci. 53*, 1−134.
18. Rokitskaya, T. I., Block, M., Antonenko, Y. N., Kotova, E. A., and Pohl, P. (2000) Photosensitizer binding to lipid bilayers as a precondition for the photoinactivation of membrane channels, *Biophys. J. 78*, 2572−2580.
19. Pohl, E. E., Peterson, U., Sun, J., and Pohl, P. (2000) Changes of intrinsic membrane potentials induced by flip-flop of long-chain fatty acids, *Biochemistry 39*, 1834−1839.
20. MacDonald, R. C., MacDonald, R. I., Menco, B. Ph. M., Takeshita, K., Subbarao, N. K., and Hu, L. R. (1991) Small-volume extrusion apparatus for preparation of large, unilammellar vesicles, *Biochim. Biophys. Acta 1061*, 297−303.
21. Mueller, P., Rudin, D. O., Tien, H. T., and Wescott, W. C. (1963) Methods for the formation of single bimolecular lipid membranes in aqueous solution, *J. Phys. Chem. 67*, 534−535.
22. Montal, M., and Mueller, P. (1972) Formation of bimolecular membranes from lipid monolayers and a study of their electrical properties., *Proc. Natl. Acad. Sci. U.S.A. 69*, 3561−3566.
23. Krylov, A. V., Pohl, P., Zeidel, M. L., and Hill, W. G. (2001) Water permeability of asymmetric planar lipid bilayers: leaflets of different composition offer independent and additive resistances to permeation, *J. Gen. Physiol. 118*, 333−340.
24. Pohl, P., Rokitskaya, T. I., Pohl, E. E., and Saparov, S. M. (1997) Permeation of phloretin across bilayer lipid membranes monitored by dipole potential and microelectrode measurements, *Biochim. Biophys. Acta 1323*, 163−172.
25. Schoch, P., Sargent, D. F., and Schwyzer, R. (1979) Capacitance and conductance as tools for the measurement of asymmetric surface potentials and energy barriers of lipid bilayer membranes, *J. Membr. Biol. 46*, 71−89.
26. Sokolov, V. S., and Kuzmin, V. (1980) Study of surface potential difference in bilayer membranes according to the second harmonic response of capacitance current, *Biofizika 25*, 170−172.
27. Harrigan, P. R., Wong, K. F., Redelmeier, T. E., Wheeler, J. J., and Cullis, P. R. (1993) Accumulation of Doxorubicin and Other Lipophilic Amines Into Large Unilamellar Vesicles in Response to Transmembrane pH Gradients, *Biochim. Biophys. Acta 1149*, 329−338.
28. Antonenko, Y. N., Denisov, G. A., and Pohl, P. (1993) Weak acid transport across bilayer lipid membrane in the presence of buffers − theoretical and experimental pH profiles in the unstirred layers, *Biophys. J. 64*, 1701−1710.
29. Dalmark, M., and Storm, H. H. (1981) A Fickian diffusion transport process with features of transport catalysis. Doxorubicin transport in human red blood cells, *J. Gen. Physiol. 78*, 349−364.
30. Kabanov, A. V., Batrakova, E. V., and Miller, D. W. (2003) Pluronic((R)) block copolymers as modulators of drug efflux transporter activity in the blood-brain barrier, *Adv. Drug Delivery Rev. 55*, 151−164.
31. Batrakova, E. V., Li, S., Alakhov, V. Y., Miller, D. W., and Kabanov, A. V. (2003) Optimal structure requirements for pluronic block copolymers in modifying P-glycoprotein drug efflux transporter activity in bovine brain microvessel endothelial cells, *J. Pharmacol. Exp. Ther. 304*, 845−854.
32. Bromberg, L., and Alakhov, V. Y. (2003) Effects of polyether-modified poly(acrylic acid) microgels on doxorubicin transport in human intestinal epithelial Caco-2 cell layers, *J. Controlled Release 88*, 11−22.
33. Schroder, G., Brandenburg, K., and Seydel, U. (1992) Polymyxin B induces transient permeability fluctuations in asymmetric planar lipopolysaccharide/phospholipid bilayers, *Biochemistry 31*, 631−638.
34. Wiese, A., Munstermann, M., Gutsmann, T., Lindner, B., Kawahara, K., Zahringer, U., and Seydel, U. (1998) Molecular mechanisms of polymyxin B Membrane interactions: Direct correlation between surface charge density and self-promoted transport, *J. Membr. Biol. 162*, 127−138.
35. Kier, L. D., Wagner, L. M., Wilson, T. V., Li, A. P., Short, R. D., and Kennedy, G. L., Jr. (1995) Cytotoxicity of ethylene oxide/propylene oxide copolymers in cultured mammalian cells, *Drug Chem. Toxicol. 18*, 29−41.
36. Batrakova, E. V., Li, S., Elmquist, W. F., Miller, D. W., Alakhov, V. Y., and Kabanov, A. V. (2001) Mechanism of sensitization of

MDR cancer cells by Pluronic block copolymers: Selective energy depletion, *Br. J. Cancer 85*, 1987−1997.

37. Kabanov, A. V., Batrakova, E. V., and Alakhov, V. Y. (2002) Pluronic block copolymers for overcoming drug resistance in cancer, *Adv. Drug Delivery Rev. 54*, 759−779.

38. Yates, S. L., Fluhler, E. N., and Lippiello, P. M. (1992) Advances in the use of the fluorescent probe fura-2 for the estimation of intrasynaptosomal calcium, *J. Neurosci. Res. 32*, 255−260.

BI035768L